Journal of Alloys and Compounds 495 (2010) 17–22

Contents lists available at ScienceDirect

Journal of Alloys and Compounds

journal homepage: www.elsevier.com/locate/jallcom

An investigation on the reaction pathway between $LiAlH_4$ and $LiNH_2$ via gaseous ammonia

Rugan Chen, Xinhua Wang*, Lixin Chen, Shouquan Li, Hongwei Ge, Yongquan Lei, Changpin Chen

Department of Materials Science and Engineering, Zhejiang University, 38 Zheda Road, Hangzhou, Zhejiang Province 310027, China

ARTICLE INFO

Article history:
Received 26 October 2009
Received in revised form 8 December 2009
Accepted 14 December 2009
Available online 23 December 2009

Keywords:
Hydrides
$LiAlH_4$
Hydrogen storage materials
Complex hydrides

ABSTRACT

Interactions between $LiAlH_4$ and $LiNH_2$ through a gaseous ammonia intermediate have been investigated. $LiAlH_4$ and $LiNH_2$ powders with a molar ratio of 1:1 were separated in two containers inside a reactor and heated from room temperature to 350 °C at a heating rate of 1 °C/min. The results showed that $LiNH_2$ would decompose into Li_2NH and NH_3 to certain extent even at a relatively low temperature. Ammonia then reacted with Al and LiH that decomposed from $LiAlH_4$, whereupon the chemical equilibrium of the system was altered and the initial reaction temperature was lowered. Ammonia decomposed from $LiNH_2$ acted as an intermediate. A pathway for the thermal decomposition of the system was proposed as:

$$LiNH_2 + LiAlH_4 \rightarrow \frac{8-3m}{10}Li_2NH + \frac{2+3m}{5}LiH + \frac{2+3m}{10}AlN + \frac{8-3m}{10}Al + \frac{48-3m}{20}H_2 \quad (0 < m < 1)$$

The heating rate and initial molar ratio of reactants will affect the value of *m*, thus the final resultants vary. The theoretical hydrogen desorption capacity of the system was calculated to be in the range of 7.39–7.88 wt.% and a total desorption capacity of 7.37 wt.% was obtained by thermal decomposition.

1. Introduction

One of the main problems of the "hydrogen economy" is finding lightweight materials that could reversibly store great amounts of hydrogen at moderate pressures and temperatures [1]. An extensive range promising materials have been investigated including Mg-compounds, amides, and complex hydrides [2]. Among these different classes of potential hydrogen storage materials, the complex hydrides, such as tetrahydroaluminates (alanates), hexahydroaluminates, amides and imides of the alkali and alkali-earths, or mixtures of these hydrides, remain attractive and continue to draw considerable interest among researchers. Alanates of the general form $MAlH_4$, where M is a lightweight alkaline metal (Li, Na or K), have a high gravimetric density of hydrogen, which is essential for their potential use as hydrogen storage materials. Among the alanates, $LiAlH_4$ is one of the most interesting compounds because of its high hydrogen-capacity (10.5 wt.%). It thermally releases hydrogen through the following three general reactions [3]:

$$LiAlH_4 \rightarrow (1/3)Li_3AlH_6 + (2/3)Al + H_2(5.3\,wt.\%H_2) \times (T = 150\text{–}175\,^\circ C) \quad (1)$$

$$Li_3AlH_6 \rightarrow 3LiH + Al + (3/2)H_2(2.6\,wt.\%H_2) \quad (T = 180\text{–}220\,^\circ C) \quad (2)$$

$$LiH + Al \rightarrow LiAl + (1/2)H_2(2.6\,wt.\%H_2) \quad (T = 400\text{–}420\,^\circ C) \quad (3)$$

The thermal decomposition temperature of $LiAlH_4$ is too high for practical use owing to thermodynamic and kinetic limitations [4]. Therefore, various strategies have been proposed and adopted to improve the hydrogen storage performance of $LiAlH_4$, such as destabilizing with metal hydrides [5,6], mechanical grinding treatment [7–9], partial cation substitution [10], and addition of catalysts [11] among others.

Lu and Fang [12] have reported that $LiAlH_4$ combined with $LiNH_2$ in a specific molar ratio without any catalysts would release a large amount of hydrogen (~8.1 wt.%) at 85–320 °C, which is much lower than the reaction temperature of reaction (1). He proposed that $LiNH_2$ reacted with LiH generated by reaction (2). Therefore, the reaction was accelerated and decomposition temperature was decreased. In contrast, Xiong et al. [13] considered that $LiAlH_4$

* Corresponding author. Tel.: +86 571 8795 2716; fax: +86 571 8795 2716.
E-mail address: xinhuawang@zju.edu.cn (X.H. Wang).

0925-8388/$ – see front matter © 2009 Elsevier B.V. All rights reserved.
doi:10.1016/j.jallcom.2009.12.081

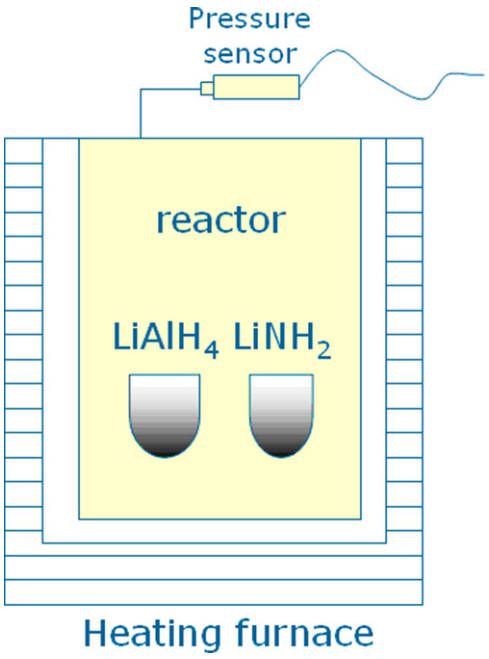

Fig. 1. Schematic diagram of the experimental device.

would react with $LiNH_2$ to form an intermediate during mechanical grinding at an ambient temperature. The chemical process for $LiAlH_4$–$LiNH_2$ interaction could be described as:

$$LiAlH_4 + LiNH_2 \rightarrow (1/3)Li_3AlH_6{-}LiNH_2{-}(2/3)Al + 2H \rightarrow [Li_2AlNH] + 5H \quad (4)$$

As reactants have a tendency to turn into amorphous crystals, some detection methods become invalid for mechanical grinding systems. With solid-state nuclear magnetic resonance (NMR) techniques, Dolotko et al. [14] confirmed the formation of AlN during mechanical grinding. A new transformation mechanism for a $LiAlH_4$–$LiNH_2$ mechanical grinding system through a series of completing solid-state processes was presented as follows:

$$2LiAlH_4(s) + LiNH_2(s) \rightarrow Li_3AlH_6 + AlN(s) + 2H_2(g) \quad (5)$$

$$Li_3AlH_6(s) + LiNH_2(s) \rightarrow 4LiH + AlN(s) + 2H_2(g) \quad (6)$$

As $LiNH_2$ is an efficient and widely used additive [15], its catalytic mechanism should be investigated thoroughly. In previously published papers, ammonia release in the $LiAlH_4$–$LiNH_2$ system is not taken into consideration, although there are considerable evidences prove that $LiNH_2$ will release ammonia when heated [16]. NH_3 will not only damage the catalyst in a fuel cell, but will also accelerate the cyclic instability of hydrogen storage materials. Therefore, reducing the ammonia emission level is important for N-containing metal complex hydrogen storage systems. The present study focuses on the role that ammonia plays and examines potential reaction pathways for the $LiAlH_4$–$LiNH_2$ system.

2. Experimental methods

The initial materials, $LiAlH_4$ (95%, CAS:16853-85-3), $LiNH_2$ (95%, CAS:7782-89-0) and AlN (98%, CAS:24304-00-5) were purchased from Aldrich Chemical and used as received, without any further purification. Influence of the impurities in the initial materials to the final experimental results was not taken into consideration. To prevent samples and raw materials from undergoing oxidation and/or hydroxide formation, they were stored and handled in an argon-filled glovebox (Mbraun MB200B). Pure $LiAlH_4$ and $LiNH_2$ with a molar ratio of 1:1 and a total weight of about 1 g were placed separately into two stainless steel containers. Both containers were placed into an airtight reactor and evacuated as shown in Fig. 1. The volume of the reactor was large enough so that the pressure variation inside the reactor would not affect the decomposition process of the reaction. The reactor was then heated from room temperature to 350 °C at a heating rate of 1 °C/min, and maintained at 350 °C for 5 h. The relationship between temperature and pressure was recorded by computer.

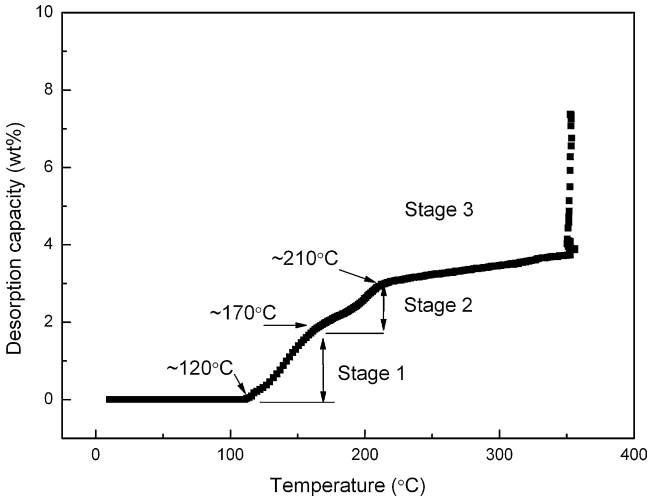

Fig. 2. Relationship between the temperature and hydrogen desorption capacity. (The reactor was heated from room temperature to 350 °C at a heating rate of 1 °C/min, and was then maintained at 350 °C for 5 h.).

The thermal gas desorption properties of the mixtures were determined by a thermogravimetry analyzer (TG) (Netzsch STA449F3) upon heating to 500 °C at a heating rate of 5 °C/min. The flow rate of argon of 99.99% purity was maintained at 40 mL/min throughout entire heating process. The outlet gas from the TG analyzer was constantly monitored using a Quadropolc Mass Spectroscopy (QMS) (Netzsch QMS 403C). The gases monitored included H_2 and NH_3. Structural analysis was carried out using a Rigaku D/max-3B X-ray diffractometer using Cu-K_α radiation at room temperature. For NMR analysis, the ^{27}Al and ^{7}Li solid-state NMR experiments were performed on a Bruker Avance II 300 MHz spectrometer. AlN(98%) from Alfa-Aesar was used as standard. The samples and the reference compounds were packed in MAS zirconia rotors in a glove box under argon atmosphere and tightly capped to minimize the possibility of oxygen contamination. The ^{27}Al and ^{7}Li shifts were referenced to 1 M aqueous solution of $Al(NO_3)_3$ and LiCl. ^{27}Al and ^{7}Li peaks of $Al(NO)_3$ and LiCl solutions were made as standard and marked as 0 ppm, respectively.

Structure analysis was carried out using a Rigaku D/max-3B X-ray diffractometer using Cu-K_α radiation at room temperature. The XRD samples were covered with a special plastic tape to prevent the contact of the sample with water vapor and oxygen.

3. Results and discussion

Fig. 2 shows the relationship between desorption capacity and temperature inside the reactor. The reaction appears to consist of three steps: the first step ranges from 120 °C to 170 °C; the second step ranges from 170 °C to 210 °C; and the third step is above 210 °C. TG–DSC analysis results of the commercial $LiNH_2$, $LiAlH_4$, and mixtures of $LiAlH_4$ and $LiNH_2$ in a molar ratio of 1:1, with and without mechanical grinding treatment, are shown in Fig. 3. The initial decomposition temperature of commercial $LiAlH_4$ is about 150 °C, which is similar to the literature value [3]. Figs. 2 and 3 clearly show that the initial decomposition temperature of the system designed in the present study is lower than that of commercial $LiAlH_4$ and $LiNH_2$. As the reactants were separated from each other, solid contact reactions could be excluded, so we consider that the NH_3 emitted by $LiNH_2$ reacted with $LiAlH_4$ (or decomposition products of $LiAlH_4$) and allowed the overall reaction to continue.

The mixture of $LiAlH_4$ and $LiNH_2$ prepared without mechanical grinding decomposed within four steps. Little weight loss of about 0.91 wt.% around 100 °C occurred during the first step owing to the mild decomposition of $LiNH_2$ (Fig. 3(c)), as the TG line of the mixture during this step was quite similar to that of commercial $LiNH_2$. The reaction characteristics of the other three steps were the same to that of commercial $LiAlH_4$, which indicates that the mixture of $LiAlH_4$ and $LiNH_2$ decomposed severally in the open

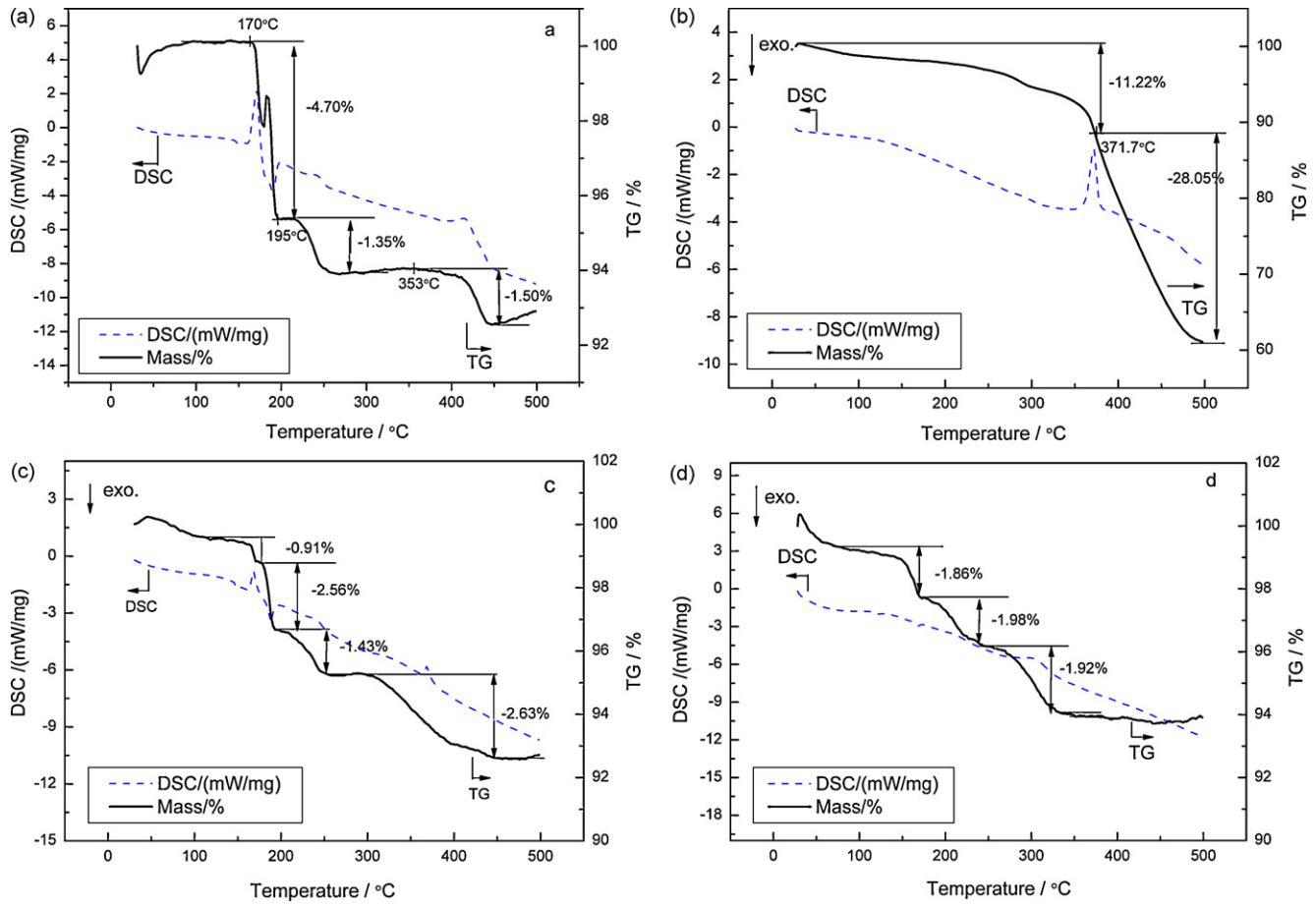

Fig. 3. TG/DSC curves of as-received $LiNH_2$ and $LiAlH_4$, and their mixture. (a) As-received $LiAlH_4$; (b) as-received $LiNH_2$; (c) mixture of $LiNH_2$ and $LiAlH_4$ in a molar ratio of 1:1 without mechanical grinding and (d) mixture of $LiNH_2$ and $LiAlH_4$ in a molar ratio of 1:1 ball milled for 3 h under Ar atmosphere.

environment because it was difficult to retain NH_3 released from $LiNH_2$ in the system. However, the mechanical grinding treatment allowed the release of a certain amount of H_2 [11,12], which suggested a solid contact reaction was taking place during mechanical grinding treatment.

These two points indicate that there are two possibilities for the reaction between $LiAlH_4$ and $LiNH_2$: through solid contact or through a gaseous ammonia intermediate. The solid contact reaction has been studied by many groups [16,17], in this paper, we focus on the gaseous ammonia reaction. In the present case, $LiAlH_4$ and $LiNH_2$ were physically separated so that the solid contact reaction was not possible. Ammonia should be the only gaseous intermediate interacting between $LiAlH_4$ and $LiNH_2$.

The endothermic peak in DSC curve of $LiNH_2$ in Fig. 3(b) reveals that $LiNH_2$ decomposes most intensely at about 372 °C, but some decomposition occurred even at relatively milder temperatures below 100 °C, as shown by its TG curve. $LiNH_2$ has been shown to decompose to a different extent across a broad temperature range between 60 °C and 500 °C [17,18], which could be described as the following reaction:

$$2LiNH_2 \rightarrow Li_2NH + NH_3 \quad (7)$$

Compared the DSC curves of the mixtures of $LiAlH_4$–$LiNH_2$ composites with the received $LiNH_2$, another phenomenon can be observed. Endothermic peaks of the mixtures corresponding to the intense decomposition of $LiNH_2$ decrease or even disappear when a mechanical grinding treatment is carried out, which indicates that $LiAlH_4$ makes the decomposition of $LiNH_2$ more continuous and efficient. Generally speaking, ammonia is harmful to hydrogen storage systems, so the ammonia release level should be strictly monitored and controlled. In the present system under study, the reaction continued with the aid of ammonia. Fig. 4 shows the composition profile of the effluent gas from the $LiAlH_4 + LiNH_2$ mixture without a mechanical grinding treatment. Peaks on the M2 (H_2) curve around 175 °C and 230 °C corresponded to the decomposition of $LiAlH_4$ and Li_3AlH_6, respectively. The NH_3 concentrations

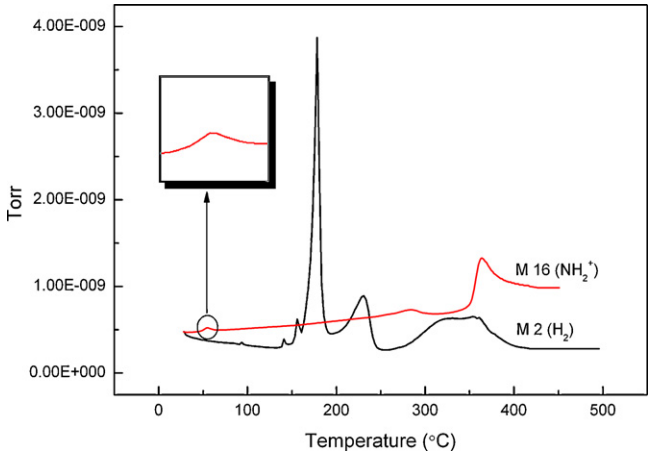

Fig. 4. The composition profile of the effluent gas released from $LiAlH_4 + LiNH_2$ mixture without mechanical grinding treatment as a function of temperature. (The heating rate is 5 °C/min with an argon flowing rate of 40 mL/min in the entire heating process.).

were quantified using the intensity of NH_2^+ species with a mass-to-charge ratio of 16. The intensity of NH_3^+ species was not used to quantify NH_3 because of the presence of OH^+ species which had the same mass-to-charge value to NH^{3+} [19]. The concentration curve for NH_2^+ exhibited a linear response to temperature as reaction temperature increased from room temperature to about 260 °C. A small peak around 60 °C was found as shown in the inner image of Fig. 4, which indicated that $LiNH_2$ could decompose slightly even at low temperature, as NH^{2+} could be ionized from NH_3 only in this system.

The X-ray diffraction pattern of $LiAlH_4$ held at 150 °C for 1 h revealed trace amounts of AlN and Li_3AlH_6. This is because ammonia released by $LiNH_2$ at low temperature can react with the Al decomposed from $LiAlH_4$. Zhang et al. [5] found that Al particles decomposed from $LiAlH_4$ to achieve an extraordinarily high dispersion over the compound and have a high activity. Our previous experiments showed that Al with high activity will react with NH_3 to form AlN and H_2. As shown in Fig. 5(c), the XRD pattern of Al powder mechanically ground under 5 atm of NH_3 atmosphere for 5 h confirmed the presence of the AlN phase. In contrast, ordinary Al powder seems to be much more stable because of the compact Al_2O_3 surface film.

Fig. 5 exhibits the XRD patterns of the products synthesized under different reaction temperatures for 1 h as shown in Fig. 1. The products of $LiAlH_4$ held at 150 °C contained a minor AlN phase, while at 200 °C, LiH, AlN and Li_3AlH_6 were found, Li_2NH and Al were detected as the reactor was heated to 300 °C. For $LiNH_2$, peaks corresponding to $LiNH_2$ decreased and ultimately disappeared as the reaction temperature increased, replaced by peaks corresponding to Li_2NH. Since commercial $LiAlH_4$ does not contain N element, the N element in $LiAlH_4$ products must have arisen from NH_3 transferred from $LiNH_2$.

As AlN presented in a predominantly amorphous form [17], the intensity of peaks corresponding to AlN was fairly low and below the limits for accurate X-ray diffraction measurement. In order to further confirm the presence of AlN, we carried out ^{27}Al measurement of probable candidates for intermediate and final products of the transformation, including initial $LiAlH_4$, and $LiAlH_4$ held at 150 °C, 200 °C and 300 °C for 1 h (heated from room temperature and then held at target temperature for 1 h). The NMR measurements shown in Fig. 6 indicate that AlN was formed when temperatures reached 150 °C and the quantity of AlN increased linearly with increase in reaction temperature. In contrast, the peak corresponding to $LiAlH_4$ decreased and ultimately vanished as transformation continued. NMR analysis of the ^7Li spectra (Fig. 6(b)) showed the formation of Li_2NH. The $LiNH_2$ sample held at 300 °C contained $LiNH_2$ and Li_2NH, which meant that $LiNH_2$ could not completely decompose into Li_2NH at 300 °C within 1 h. In other words, the reaction kinetics was relatively slow.

Based on this analysis, we divide the reaction process into three stages, as shown in Fig. 2. The transformation occurring in Stage I can be described as follows:

$$LiAlH_4 \rightarrow Li_3AlH_6 + (1/3)Al + H_2 \quad (8)$$

$$LiNH_2 \rightarrow (1/2)Li_2NH + (1/2)NH_3 \quad (9)$$

$$Al + NH_3 \rightarrow AlN + (3/2)H_2 \quad (10)$$

The wave line of the TG curve in Fig. 3(a) represents the melting of $LiAlH_4$. The melting point of $LiAlH_4$ is close to the decomposition temperature of Li_3AlH_6 [3], at about 170 °C. Residual $LiAlH_4$ started to melt at Stage II, as temperature reached the melting point. At the same time, Li_3AlH_6 acting as an intermediate decomposed according to reaction (2). The decomposition products of Li_3AlH_6 consisted of Al, H_2 and LiH. Leng et al. have reported that LiH quickly reacts with NH_3, even at room temperature [19]. The NH_3 produced from $LiNH_2$ decomposition reacted simultaneously with Al and LiH to form Li_2NH and AlN at Stage II. Because the decomposition process of $LiNH_2$ was dependent on the chemical equilibrium, the decomposition of $LiNH_2$ could not proceed rapidly enough. The XRD pattern of the $LiAlH_4$ products at Stage II (Fig. 5(a), 200 °C) revealed a small amount of $LiAlH_4$, Li_2NH and Li_3AlH_6. As previously mentioned, commercial $LiAlH_4$ powder contains no N element, so

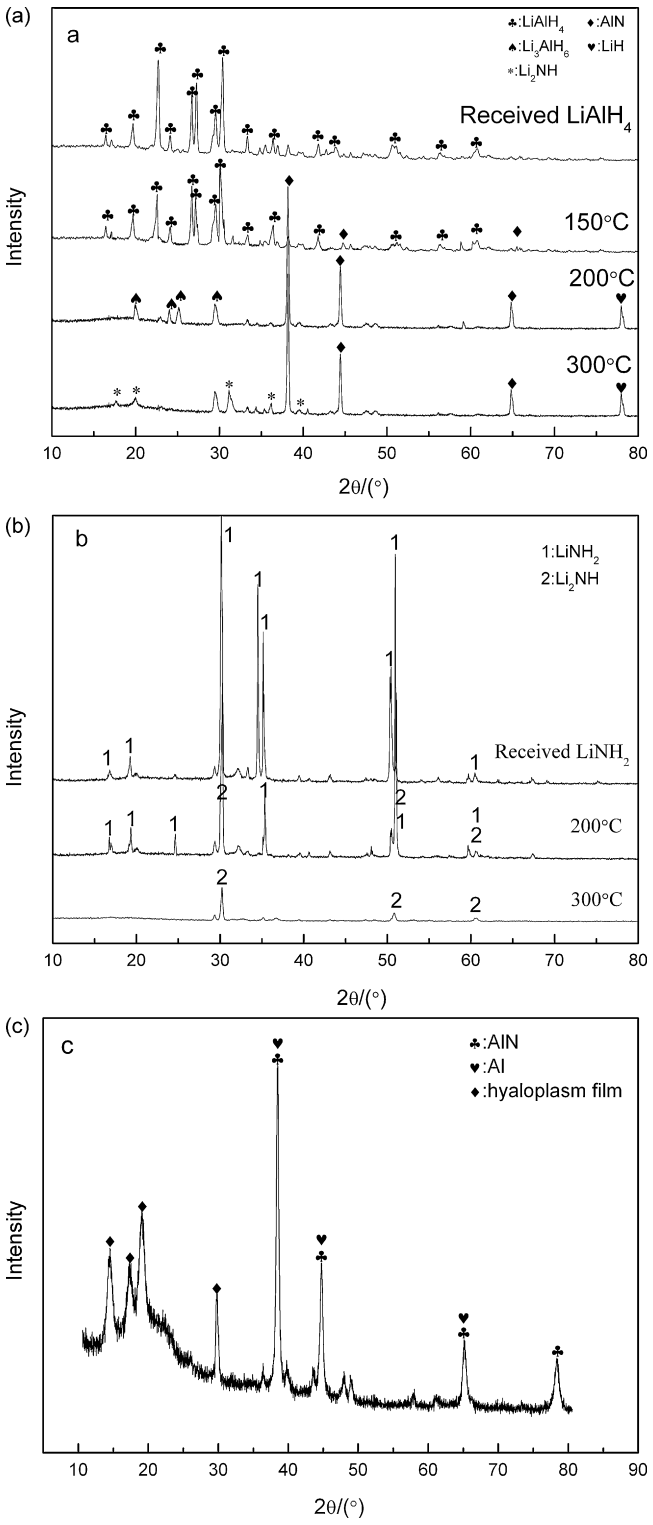

Fig. 5. XRD patterns of reactants and resultants synthesized at different temperatures. (a) Resultants of $LiAlH_4$ at 150 °C, 200 °C and 300 °C for 1 h; (b) resultants of $LiNH_2$ at 200 °C and 300 °C for 1 h and (c) Al powder ball milled under 5 atm of NH_3 for 5 h.

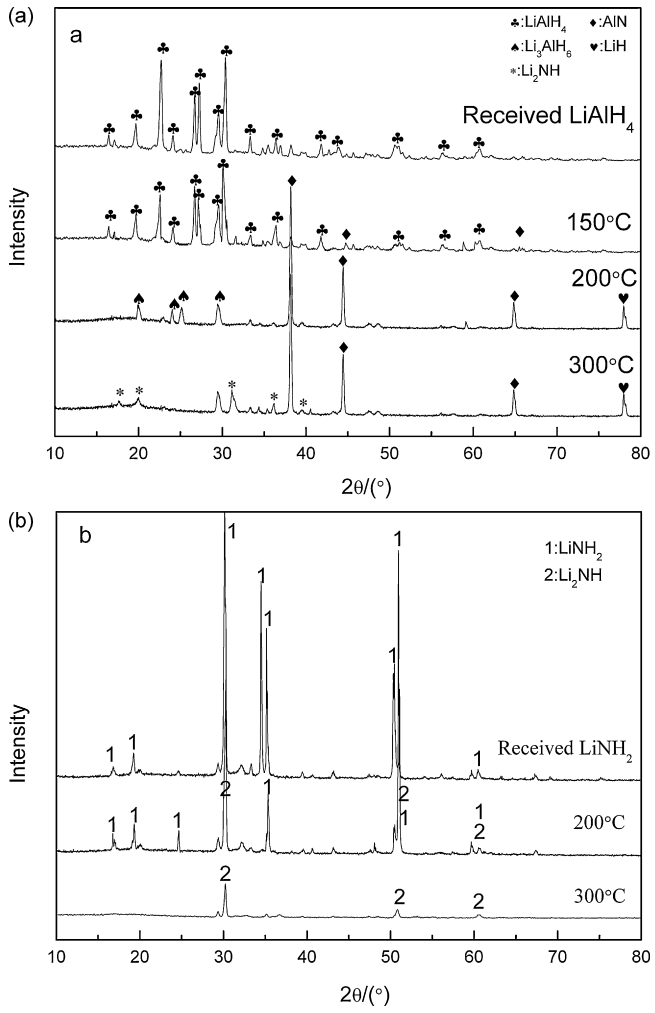

Fig. 6. ^{27}Al and ^{7}Li MAS NMR spectra of the mixture of $LiAlH_4$ + $LiNH_2$ kept at different temperatures for 1 h. (a) ^{27}Al MAS NMR spectra and (b) ^{7}Li MAS NMR spectra.

the N element seen here must have been transferred from $LiNH_2$ by a gaseous ammonia intermediate. The X-ray diffraction measurements confirmed the decreasing in $LiNH_2$ associating with the increasing of Li_2NH as the temperature was increased. The main reaction taking place at Stage II can be described as follows.

Residual $LiAlH_4$ will decompose completely at Stage II.

$$LiAlH_4 \rightarrow Li_3AlH_6 + (1/3)Al + H_2 \quad (11)$$

Decomposition of $LiNH_2$ will not be complete, as the XRD pattern showed massive amounts of $LiNH_2$ at 200 °C.

$$LiNH_2 \rightarrow (1/2)Li_2NH + (1/2)NH_3 \quad (12)$$

Al and LiH decomposed from Li_3AlH_6 react with NH_3 to form AlN and $LiNH_2$, this reaction between NH_3 and Li_3AlH_6 may be generalized as:

$$Li_3AlH_6 + (5/2)NH_3 \rightarrow AlN + (3/2)Li_2NH + 6H_2 \quad (13)$$

At Stage III, the situation is quite simple. Residual Li_3AlH_6 and $LiNH_2$ will decompose completely. Li_2NH is quite stable at 350 °C, so the main reactions at Stage III could be written as follows:

$$LiNH_2 \rightarrow (1/2)Li_2NH + (1/2)NH_3 \quad (14)$$

Ammonia then reacts with Li_3AlH_6 to form AlN and Li_2NH as follows:

$$Li_3AlH_6 + (5/2)NH_3 \rightarrow AlN + (3/2)Li_2NH + 6H_2 \quad (15)$$

Since the molar ratio of $LiNH_2$ and $LiAlH_4$ is 1:1, it can be calculated that Li_3AlH_6 is present in excess. The total quantity of Li_3AlH_6 is one-third that of $LiAlH_4$ according to reaction (1). Therefore, residual Li_3AlH_6 likewise decomposes at Stage III, as follows:

$$Li_3AlH_6 \rightarrow 3LiH + Al + (3/2)H_2 \quad (16)$$

Combining all of these reactions, an overall reaction can be written to characterize the entire transformation of $LiNH_2$ and $LiAlH_4$ in the present system as:

$$LiNH_2 + LiAlH_4 \rightarrow \frac{8-3m}{10}Li_2NH + \frac{2+3m}{5}LiH + \frac{2+3m}{10}AlN + \frac{8-3m}{10}Al + \frac{48-3m}{20}H_2 \quad (0 < m < 1)$$

where m represents the percentage of decomposing of $LiNH_2$ at Stage I.

We repeatedly affirmed that the transformation of the system was dominated by the chemical equilibrium, so the decomposition process for $LiNH_2$ is likely to be slow and continuous. Therefore, the heating rate and reaction temperature will have substantial effects on the value of m. Different heating rates will result in different products. On the whole, the theoretical hydrogen releasing capacity should be in the range of 7.39–7.88 wt.% as molar ratio of $LiAlH_4$ and $LiNH_2$ is 1:1. A total hydrogen desorption capacity of 7.37 wt.% was obtained (Fig. 2), which is close to the theoretical calculation. The total weight loss in TG test was about 7.53 wt.%, which is higher than the data obtained by the thermal desorption experiment. The reason for this phenomenon may be attributable to the different end temperatures, which were 500 °C for TG analysis, but only 350 °C for the thermal desorption.

4. Conclusions

An interaction between $LiAlH_4$ and $LiNH_2$ through a gaseous ammonia intermediate was studied. $LiNH_2$ may release ammonia across a broad range of temperatures, which reacts with Al and LiH decomposed from $LiAlH_4$. Ammonia is continuously produced and then consumed, making the whole reaction sustains. Because the decomposition of $LiNH_2$ is dominated by the chemical equilibrium, the whole reaction is slow and incomplete. The overall reaction can be expressed as:

$$LiNH_2 + LiAlH_4 \rightarrow \frac{8-3m}{10}Li_2NH + \frac{2+3m}{5}LiH + \frac{2+3m}{10}AlN + \frac{8-3m}{10}Al + \frac{48-3m}{20}H_2 \quad (0 < m < 1)$$

where m represents the decomposition percentage of $LiNH_2$ when the temperature is below 170 °C (Stage I). The heating rate and initial molar ratio of $LiNH_2$ and $LiAlH_4$ in the system will affect the m value, so the final products may be different. The theoretical desorption capacity is calculated to range from 7.39% to 7.88% as m varies. A total hydrogen desorption capacity of 7.37 wt.% was obtained when $LiNH_2/LiAlH_4$ was heated from room temperature to 350 °C with a heating rate of 1 °C/min and maintained at the final temperature for 5 h.

Acknowledgment

This work was supported by National Natural Science Foundation of China (Nos. 50671094 and 50631020) and National Basic Research Program of China (Nos. 2007CB209706 and 2010CB631304).

References

[1] L. Schalappabach, A. Züttel, Nature 414 (2001) 353–358.

[2] A. Zaluska, L. Zaluski, J.O. Strŏm-Olsen, J. Alloys Compd. 288 (1–2) (1999) 217–225.
[3] L. Hima Kumar, B. Viswanathan, S. Srinvivasa Murthy, Int. J. Hydrogen Energy 33 (2008) 366–373.
[4] J.W. Jang, J.H. Shim, Y.W. Cho, B.J. Lee, J. Alloys Compd. 420 (1–2) (2006) 286–290.
[5] Y. Zhang, Q.F. Tian, S.S. Liu, L.X. Sun, J. Power Sources 185 (2008) 1514–1518.
[6] A.W. Vittetoe, M.U. Niemann, S.S. Srinivasan, K. McGrath, A. Kumar, D.Y. Goswami, E.K. Stefanakos, S. Thomas, Int. J. Hydrogen Energy 34 (2009) 2333–2339.
[7] L. Zaluski, A. Zaluska, J.O. Strŏm-Olsen, J. Alloys Compd. 290 (1–2) (1999) 71–78.
[8] H.W. Brinks, B.C. Hauback, C.M. Jensen, R. Zidan, J. Alloys Compd. 392 (1–2) (2005) 27–30.
[9] A. Zaluska, L. Zaluski, J.O. Strŏm-Olsen, J. Alloys Compd. 298 (1–2) (2000) 125–134.
[10] Y. Nakamori, S. Orimo, Mater. Sci. Eng. B 108 (1–2) (2004) 48–50.
[11] T. Sun, C.K. Huang, H. Wang, L.X. Sun, M. Zhu, Int. J. Hydrogen Energy 33 (2008) 6216–6221.
[12] J. Lu, Z.G.Z. Fang, J. Phys. Chem. 109 (2005) 20830–20834.
[13] Z.T. Xiong, G.T. Wu, J.J. Hu, P. Chen, J. Power Sources 159 (2006) 167–170.
[14] O. Dolotko, H.Q. Zhang, O. Ugurlu, W.W. Jerzy, M. Pruski, S.L. Chumbley, V. Pecharsky, Acta Mater. 55 (2007) 3121–3130.
[15] T. Noritake, M. Aoki, S. Towata, A. Ninomiya, Y. Nakamor, Appl. Phys. A 83 (2006) 277–279.
[16] W.F. Luo, K. Stewart, J. Alloys Compd. 440 (2007) 357–361.
[17] Y.H. Hu, E. Ruckenstein, Ind. Eng. Chem. Res. 42 (2003) 5135–5139.
[18] L. Shaw, R. Ren, T. Markmaitree, W. Osborn, J. Alloys Compd. 448 (2007) 263–271.
[19] H.Y. Leng, T. Ichikawa, S. Hino, N. Hanada, S. Isobe, H. Fuji, J. Power Sources 156 (2006) 166–170.